ELSEVIER

A theoretical study of the response of vascular tumours to different types of chemotherapy

Jasmina Panovska[a,*], Helen M. Byrne[b], Philip K. Maini[c]

[a] *Chemical Engineering, Heriot-Watt University, Riccarton Campus, Edinburgh, EH14 4AS, UK*
[b] *Centre for Mathematical Medicine, School of Mathematical Sciences, University of Nottingham, Nottingham, NG7 2RD, UK*
[c] *Centre for Mathematical Biology, Mathematical Institute, Oxford University, Oxford OX1 3LB, UK*

Abstract

In this paper we formulate and explore a mathematical model to study continuous infusion of a vascular tumour with isolated and combined blood-borne chemotherapies. The mathematical model comprises a system of nonlinear partial differential equations that describe the evolution of the healthy (host) cells, the tumour cells and the tumour vasculature, coupled with distribution of a generic angiogenic stimulant (TAF) and blood-borne oxygen. A novel aspect of our model is the presence of blood-borne chemotherapeutic drugs which target different aspects of tumour growth (cf. proliferating cells, the angiogenic stimulant or the tumour vasculature). We run exhaustive numerical simulations in order to compare vascular tumour growth before and following therapy. Our results suggest that continuous exposure to anti-proliferative drug will result in the vascular tumour being cleared, becoming growth-arrested or growing at a reduced rate, the outcome depending on the drug's potency and its rate of uptake. When the angiogenic stimulant or the tumour vasculature are targeted by the therapy, tumour elimination can not occur: at best vascular growth is retarded and the tumour reverts to an avascular form. Application of a combined treatment that destroys the vasculature and the TAF, yields results that resemble those achieved following successful treatment with anti-TAF or anti-vascular therapy. In contrast, combining anti-proliferative therapy with anti-TAF or antivascular therapy can eliminate the vascular tumour. In conclusion, our results suggest that tumour growth and the time of tumour clearance are highly sensitive to the specific combinations of anti-proliferative, anti-TAF and anti-vascular drugs.
© 2008 Published by Elsevier Ltd

Keywords: Vascular tumour; Single and combined therapy

1. Introduction

Tumour growth is a complex process that involves a sequence of well-orchestrated events. These include the initial avascular phase of growth, angiogenesis, the process by which the tumour becomes vascularized, and the vascular phase of growth. During the early growth stage, oxygen and other nutrients are delivered to the tumour cells, and the waste products are removed from the tumour, via diffusion from nearby blood vessels, the tumour cells proliferate

---

rapidly consuming more oxygen than the host cells [1]. Due to diffusion limited supply of nutrients initial (avascular) growth is limited in size [2]. To grow larger the tumour must complete a sequence of processes that include the secretion of TAFs, such as vascular endothelial growth factor (VEGF) and initiate the angiogenic process. During angiogenesis VEGF stimulates the formation of a tumour-specific vascular network from the host vessels. Upon successful vascularization oxygen is rapidly supplied to the tumour by the neovasculature so it can grow larger and metastasize. Tumours generally become vascularized after approximately 14–21 days [3] and are usually detectable only after they have vascularized and grown larger invading the adjacent healthy tissue.

Thus far it has proved difficult to find a treatment that can control all aspects of tumour growth. In different stages of growth different treatments can be relevant. For example, to prevent tumour vascularization, anti-TAF drugs can be administered or antivascular drugs would aim to kill the neovasculature during angiogenesis. Alternatively, due to excessive proliferation of tumour cells anti-proliferative treatments are also relevant. An ideal treatment would control tumour invasion, remove all the tumour cells from the affected region and prevent further tumour cell production, whilst inflicting no damage to the normal tissue [4]. Due to the complexity of tumour growth this is usually not possible and currently available tumour therapies include surgical intervention [5], exposure to radiation or laser treatment [6], and injection of anticancer drugs into the bloodstream or the surrounding normal tissue [4].

The aim of surgery is to remove as much of the tumour as possible together with the associated blood supply to arrest its progression. Surgery can also be undertaken as a preventative measure to remove tissue that is not cancerous but is likely to become so. For example, preventative surgery is used to remove precancerous polyps in the colon [5]. Curative surgery involves the removal of tumours that are confined to one area; it is the main treatment for primary tumours that have not metastasized. Unfortunately, many cancers are inoperable due to their location, for example, severe forms of brain tumours [7]. Further, surgery is often undesirable as it is a traumatic process that poses particular risks to elderly and infirm patients.

Radiation therapy (known as radiotherapy) has long been used to eradicate various tumours, especially those in internal organs, lymphomas and cancers of the prostate [6]. High-powered radiation rays damage tumour cells and thereby prevent the tumour from growing. Radiotherapy is often used to destroy tumour tissue that cannot be removed with surgery or to target cancer cells that may remain after surgery. Doctors and scientists are continually striving to improve radiation techniques. Some of the suggested improvements are 3D-imaging where doctors can more accurately view the tumour mass before to radiation [8] and then focus the radiation at a specific location [9].

Chemotherapy is perhaps the most common anticancer treatment. Treatment may consist of a single drug or a combination, usually delivered orally or by injection [4,7]. Drugs that act on tumour cells can be subdivided into those that target both proliferating and nonproliferating (quiescent) cells in different parts of the tumour mass, and those that target only dividing cells in specific phases of cell division [10]. Some drugs not only kill cancer cells, but can also kill rapidly dividing non-cancerous (host) cells. For example, hair follicles are extinguished, causing severe hair loss in chemotherapy patients [11]. The reason that this treatment is feasible is that following treatment normal tissue may recover fully whilst the tumour will be removed. A common type of chemotherapy drugs are cell-cycle-specific chemotherapy drugs such as cyclophosphamide [12] which acts upon cells in the DNA replication phase of the cycle, or Taxol [13] which more effectively influence cells in the division phase of the cell cycle.

A more recent treatment involves applications which either target tumour angiogenic factors (TAFs) or attack the new capillaries. Since, in practice a tumour is usually already vascularized when detected, such antiangiogenic therapies are likely to be effective. For example thalidomide is an antiangiogenic drug which acts by inhibiting endothelial cell growth and has shown promising results when used to treat kidney tumours [14]. Combretastatin is another antiangiogenic drug that is currently in clinical trials and works by causing the immature vasculature inside the solid tumour to collapse [15].

The treatments mentioned above used to date have proved to be highly variable from one patient to another. One of the main reasons for this high variability is the issue of toxicity of the drugs. Namely, there is a lack of patient volunteers for *in vivo* clinical trials of new drugs, so many drugs can only be tested in small animals (e.g. mice). Although successful here, these drugs may be toxic to the human patient and therefore result in disastrous side-effects. The delivery of the treatment is also relevant: sometimes when the drugs are delivered to the tumour they can bypass large areas of the target. In order to facilitate clinical studies of tumour treatments, theoretical models are being developed. These models can be formulated in a mathematical framework and are being viewed as a technique that can complement medical studies in the quest to halt tumour growth. Mathematical modelling can be used to compare different treatment protocols and has the potential to reduce significantly the time and money needed to develop and

test new drugs. This can be achieved by performing numerical simulations of mathematical models in which new drugs are tested and optimal protocols determined before being used to guide clinical trials. Mathematical models may also be used to suggest the existence of new mechanisms to explain observed clinical phenomena. In some respects it is the predictive capability of mathematical models that is their most important feature.

Within the last three decades a number of mathematical models for tumour growth have been developed. Most models focus on one particular aspect, for example, avascular growth (e.g. [16,17]), tissue interactions (e.g. [18,19]), angiogenesis (e.g. [20–23]) or vascular tumour growth (e.g. [24–27]). In [28] we formulated and studied a continuum model that can describe tumour development from the avascular growth phase through tumour angiogenesis to the vascular growth phase. The novel aspect of the model developed in [28] was the coupling between the cell densities, the oxygen concentration and the vasculature. For example, when the oxygen concentration falls to low values, tumour cells (and to a lesser extent normal cells) secrete TAFs such as the vascular endothelial growth factor (VEGF) that initiate the angiogenic process [29]. This coupling distinguishes our model from existing models of tumour–host interaction [18], tumour angiogenesis [21] and previous models of vascular growth such as [30]. In this paper we extend our earlier model to compare the effect of different drugs on tumour growth.

We do this by incorporating an equation for a generic drug delivered to the tumour by the vasculature. The drug targets either proliferating cells (cf. doxorubicin [31]), or the angiogenic process (e.g. reduce the influence of VEGF) or kill the tumour neovasculature. In [28] it was assumed that both tumour and healthy host cells proliferate, and that cells constituting the vasculature simply migrated towards the VEGF source without proliferating. This assumption was based on observations by Sholley and Ferguson [32] which showed that the migration of capillary tips towards VEGF is essential for successful angiogenesis and that proliferation within the capillary tips is less important. Thus, in our model, a drug with anti-proliferative properties targets only tumour and normal cells. For future reference, we call this "drug A". Another key aspect of tumour growth is angiogenesis. Drugs that target this process aim either to reduce the strength of the angiogenic stimuli (VEGF in our case) (cf. inhibitors such as endostatin [33] or angiostatin [34]), or to target directly the angiogenic capillary tips (cf. combretastatin [35]). For the rest of this paper we term a drug that reduces the strength of the VEGF field as "drug B", and a drug that targets the angiogenic capillary tips as "drug C". We will also study the effect of a drug that reduces the blood vessel density by targeting the blood vessels that produce the angiogenic tips in the tissue surrounding the tumour. We refer to such a drug as "drug D" but note, to our knowledge, that such a drug is not currently available. We use our simulations to compare its effect against the effects of drugs A–C.

The incorporation of drugs A–D distinguishes our work from previous chemotherapy models where only one type of drug was studied. For example, models that studied the effect of drugs of type A have been developed by Ward and King [36] and Jackson and Byrne [37]. The former model explored the effect of chemotherapy on the rate of tumour growth in multicellular spheroid and mono-layer cultures, whereas Jackson and Byrne [37] studied the effect of blood-borne chemotherapy on two cell types, one of which is more resistant to the drug. Other authors have explored the effect of drugs that target the angiogenic stimulus (VEGF) (type B) [26,27] or drugs of types C and D that destroy (immature and mature) tumour vessels [38,39].

A different therapeutic approach was taken by Sinek et al. [40]. They have recently extended the model of Zheng et al. [41] to develop a multiscale tumour simulator to study the effect of chemotherapy on tumour progression through its avascular and vascular growth stages. They performed 2-D simulations based on a self-consistent parameter estimation that demonstrated the fundamental convective and diffusive transport limitations in delivering anticancer drug into tumours regardless of whether this delivery was via free drug administration (e.g. intravenous drip), via 100 nm nanoparticles injected into the bloodstream, extravasating and releasing the drug that then diffused into the tumour, or via smaller 1–10 nm nanoparticles capable of diffusing directly and targeting the individual tumour cell. The results predicted that even in a best-case scenario, involving constant drug release from the nanoparticles and a homogeneous, not drug resistant tumour of one cell type, the fundamental transport limitations were severe and drug levels inside the tumour were far less than *in vitro*, leaving large parts of the tumour with inadequate drug concentration.

Cancer chemotherapies have also been studied by Fister and Penetta [42,43]. They used a system of ordinary differential equations and optimal control techniques to develop optimal strategies for chemotherapy. In particular, the authors investigated the qualitative differences between three different cell-kill models: log-kill hypothesis (cell-kill proportional to mass); Norton–Simon hypothesis (cell-kill proportional to growth rate) and Emax hypothesis (cell-kill proportional to a saturable function of mass). For each hypothesis, an optimal drug strategy was characterized that minimized the cancer mass and the cost (in terms of total amount of drug). Their work modelled well-established drugs

such as metha-trexate, which has been used to treat leukemia in the last 30 years, as well as more speculative drugs which are currently unavailable [43]. Their numerical results showed the qualitatively different treatment schemes for each hypothesis. In particular, they predicted that the log-kill hypothesis required less drug compared to the Norton–Simon hypothesis to reduce the cancer an equivalent amount over the treatment interval.

In contrast to the spatially-averaged models developed by Sinek et al. [40] or Fister et al. [42,43] we use non-linear partial differential equations to study the response of vascular and avascular tumours to different chemotherapeutic drugs. The structure of this paper is as follows. In Section 2, we introduce our mathematical model, focusing our description on the drug and how it is incorporated into our earlier model of vascular tumour growth. We briefly recap our results from [28] in Section 3. In Sections 4–6 we illustrate the types of behaviour that result when a one-dimensional tumour is exposed to a single chemotherapeutic drug. The tumour's response to combinations of these drugs is investigated in Sections 7 and 8. Finally, we present our conclusions and comment on future research directions in Section 9.

2. Mathematical model

In this section we extend the mathematical model for vascular tumour growth from [28] to include an equation for a blood-borne therapeutic drug with different modes of action. We recall that tumour growth, via invasion of the surrounding host cells and angiogenesis, is a multi-dimensional process. In this paper, however, as in [28], we average the dependent variables in a plane perpendicular to the direction of the invasion of the tumour front and we restrict attention to one spatial dimension. This direction is chosen to be parallel to the line connecting the limbus, situated at $x = 0$ and where the nearest host blood vessels are found, to the tumour centre at $x = 1$ (in dimensionless terms). We introduce independent variables t and x representing, respectively, time and spatial position in a direction parallel to that of tip growth.

Within our modelling framework we consider two types of dependent variables: those that contribute to the tumour volume and those of negligible volume. The former category comprise the healthy (host) cell density $n_1(x, t)$, the tumour cell density $n_2(x, t)$, the capillary tip density $n_3(x, t)$ and the density of the blood vessels $b(x, t)$. Variables of negligible volume are the nutrient concentration $a(x, t)$ (here taken to be oxygen), the TAF concentration $c(x, t)$ (here vascular endothelial growth factor (VEGF)) and the drug concentration $d(x, t)$.

We now describe these equations, noting that details can be found in [28].

Following [18], in the absence of therapy, we use nonlinear reaction–diffusion equations to model the tumour and normal cell densities. We also assume that the normal tissue is immobile. As in [18] we assume that the tumour is unable to spread unless the surrounding healthy tissue is below its carrying capacity. Thus the expansion of the tumour into the adjacent tissue depends on its composition and we assume that the random motion coefficient for the tumour cell density depends on the density of the surrounding normal cells. We also include competition between the host and the tumour cells for space and oxygen through simple Lotka–Volterra competition. Unlike [18], the equations we use for the tumour and the host cell density are coupled via the oxygen equation, rather than hydrogen ion density H^+ (the latter provides a measure of the local pH). We assume that oxygen is blood-borne and that it controls cell proliferation and cell death. These assumptions are based on experimental observations of tumour–host interactions in the presence and absence of oxygen [1]. Following [44,21], and as in [28] we use the 'snail-trail' modelling of fungal growth [45] to describe the interactions between the vasculature and the VEGF. We assume that tip cells dictate the movement of the vascular front. One novel feature of [28] was the introduction of a nonlinear chemotaxis coefficient to describe capillary tip movement towards the tumour. We keep this assumption here also. The branching of the blood vessels is influenced by VEGF and leads to the production of capillary tips. We incorporate vessel remodelling by including logistic growth in Eq. (6). The key assumption in the model from [28] is that hypoxic cells secrete VEGF and this initiates the angiogenic process. Thus Eqs. (1)–(3) couple to Eqs. (4)–(6) via the blood-borne delivery of oxygen in (3) and also the assumed production of VEGF by the tumour and normal cells under low oxygen (see Eq. (4)). We summarize the (dimensionless) equations for the host $n_1(x, t)$ and the tumour $n_2(x, t)$ cell densities, the oxygen concentration $a(x, t)$, the capillary tip density $n_3(x, t)$, the blood vessel density $b(x, t)$ and the VEGF concentration $c(x, t)$ as follows:

$$\frac{\partial n_1}{\partial t} = \frac{r_1 \rho_1 a}{1 + \rho_1 a} n_1 - r_1 n_1^2 - \frac{R_1 n_1}{1 + \rho_1 a} - c_1 n_1 n_2, \tag{1}$$

$$\frac{\partial n_2}{\partial t} = \frac{\partial}{\partial x}\left(d_{n_2}(1 - n_1)\frac{\partial n_2}{\partial x}\right) + \frac{r_2\rho_2 a}{1 + \rho_2 a}n_2 - r_2 n_2^2 - \frac{R_2 n_2}{1 + \rho_2 a} - c_2 n_1 n_2, \tag{2}$$

$$\frac{\partial a}{\partial t} = d_a\frac{\partial^2 a}{\partial x^2} + hb(1 - a) - \frac{\lambda_1 r_1 a n_1}{1 + \rho_1 a} - \frac{\lambda_2 r_2 a n_2}{1 + \rho_2 a}, \tag{3}$$

$$\frac{\partial c}{\partial t} = d_c\frac{\partial^2 c}{\partial x^2} + \frac{r_3}{1 + \rho_1 a}n_1 + \frac{r_4}{1 + \rho_2 a}n_2 - p_1 bc - \gamma c, \tag{4}$$

$$\frac{\partial n_3}{\partial t} = d_{n_3}\frac{\partial^2 n_3}{\partial x^2} - \frac{\partial}{\partial x}\left(\frac{\psi c}{1 + \eta c}n_3\frac{\partial c}{\partial x}\right) + p_2 bc - \beta_1 n_3 b, \tag{5}$$

$$\frac{\partial b}{\partial t} = d_{n_3}\frac{\partial n_3}{\partial x} - \frac{\psi c}{1 + \eta c}n_3\frac{\partial c}{\partial x} + s_1 b(1 - b) - \delta b. \tag{6}$$

and we refer the reader to [28] for further details.

In order to study the effect of therapy on vascular tumour growth, we now couple Eqs. (1)–(6) with an equation for a generic drug $d(x, t)$. We assume that the spatiotemporal evolution of the drug concentration is influenced by diffusion, its delivery by the vessels and its loss due to uptake by the relevant cells. In dimensionless terms we write (see [46] for more details)

$$\epsilon_d\frac{\partial d}{\partial t} = \frac{\partial^2 d}{\partial x^2} + \Gamma b(1 - d) - \frac{\beta_1\rho_5 n_1}{1 + \rho_5 n_1}d - \frac{\beta_2\rho_6 n_2}{1 + \rho_6 n_2}d - \beta_3 cd - \frac{\beta_4\rho_5 n_3}{1 + \rho_5 n_3}d - \frac{\beta_5\rho_5 b}{1 + \rho_5 b}d - \lambda_3 d.$$

We model drug delivery by the vasculature using the source term $\Gamma b(1 - d)$ which is similar to the source term in (3). Depending on which of drugs A–D we are studying, different sink terms are present in (7). When drug A is being used the terms $\frac{\beta_1\rho_5 n_1}{1 + \rho_5 n_1}d$ and $\frac{\beta_2\rho_6 n_2}{1 + \rho_6 n_2}d$ describe its uptake at rates β_1 and β_2 by the normal and tumour cells respectively (see Table 1). Similarly $\beta_3 cd$ represents the rate at which drug B is neutralized by VEGF, and the term $\frac{\beta_4\rho_5 n_3}{1 + \rho_5 n_3}d$ is used when drug C is being studied. For drug D the term $\frac{\beta_5\rho_5 b}{1 + \rho_5 b}d$ describes its uptake by endothelial cells that line the blood vessels. Finally, in (7) we assume that, regardless of its type, the drug undergoes natural decay at rate λ_3.

To complete our model we now modify Eqs. (1)–(7) to account for the action of the drug, the term that is active depending on whether drug A, B, C or D is being used. When drugs A, B, C or D are used, additional sink terms are included in the Eqs. (1) and (2), (4) and (5) or (6) as appropriate. We assume that these sink terms are proportional to the sink terms in (7) that describe the uptake or neutralization of drugs A–D by the appropriate variables on which they act (cells, VEGF or vessels). The functional forms for the therapeutic effect are included in Table 1. We note that the parameters Δ_i ($i = 1, 2, \ldots, 5$) represent the maximum potency whereas ρ_i ($i = 1, 2, \ldots, 5$) represent the sensitivity of drugs A–D on the normal and tumour cells, VEGF, angiogenic capillaries or the blood vessels respectively (see Table 1).

Incorporating the features outlined in Table 1 into Eqs. (1)–(6) we arrive at the following nondimensionalized system of equations:

$$\frac{\partial n_1}{\partial t} = \frac{r_1\rho_1 a}{1 + \rho_1 a}n_1 - r_1 n_1^2 - \frac{R_1 n_1}{1 + \rho_1 a} - c_1 n_1 n_2 - \underbrace{\frac{\Delta_1\rho_5 n_1}{1 + \rho_5 n_1}d}_{\text{drug A}}, \tag{7}$$

$$\frac{\partial n_2}{\partial t} = \frac{\partial}{\partial x}\left(d_{n_2}(1 - n_1)\frac{\partial n_2}{\partial x}\right) + \frac{r_2\rho_2 a}{1 + \rho_2 a}n_2 - r_2 n_2^2 - \frac{R_2 n_2}{1 + \rho_2 a} - c_2 n_1 n_2 - \underbrace{\frac{\Delta_2\rho_6 n_2}{1 + \rho_6 n_2}d}_{\text{drug A}}, \tag{8}$$

$$\frac{\partial a}{\partial t} = \frac{\partial^2 a}{\partial x^2} + hb(1 - a) - \frac{\lambda_1\rho_1 a n_1}{1 + \rho_1 a} - \frac{\lambda_2\rho_2 a n_2}{1 + \rho_2 a}, \tag{9}$$

$$\frac{\partial c}{\partial t} = d_c\frac{\partial^2 c}{\partial x^2} + \frac{r_3}{1 + \rho_1 a}n_1 + \frac{r_4}{1 + \rho_2 a}n_2 - p_1 bc - \gamma c - \underbrace{\Delta_3 cd}_{\text{drug B}}, \tag{10}$$

Table 1
Summary of the action of different drugs

Drug	Target	Example of real drug with similar properties	Potency effect (functional form)	Drug uptake (functional form)
A	Proliferating cells	Doxorubicin [49,51]	$\frac{\Delta_1\rho_5 n_1}{1+\rho_5 n_1}d$, $\frac{\Delta_2\rho_6 n_2}{1+\rho_6 n_2}d$	$\frac{\beta_1\rho_5 n_1}{1+\rho_5 n_1}$, $\frac{\beta_2\rho_6 n_2}{1+\rho_6 n_2}d$
B	VEGF	Thrombospondin [53]	$\Delta_3 cd$	$\beta_3 cd$
C	Angiogenic capillaries	Combretastatin [35]	$\frac{\Delta_4\rho_5 n_3}{1+\rho_5 n_3}d$	$\frac{\beta_4\rho_5 n_3}{1+\rho_5 n_3}d$
D	Blood vessels	Not known	$\frac{\Delta_5\rho_5 b}{1+\rho_5 b}d$	$\frac{\beta_5\rho_5 b}{1+\rho_5 b}d$

$$\frac{\partial n_3}{\partial t} = d_{n_3}\frac{\partial^2 n_3}{\partial x^2} - \frac{\partial}{\partial x}\left(\frac{\psi c}{1+\eta c}n_3\frac{\partial c}{\partial x}\right) + p_2 bc - \beta n_3 b - \underbrace{\frac{\Delta_4\rho_5 n_3}{1+\rho_5 n_3}d}_{\textbf{drug C}}, \tag{11}$$

$$\frac{\partial b}{\partial t} = d_{n_3}\frac{\partial n_3}{\partial x} - \frac{\psi c}{1+\eta c}n_3\frac{\partial c}{\partial x} + s_1 b(1-b) - \delta b - \underbrace{\frac{\Delta_5\rho_5 b}{1+\rho_5 b}d}_{\textbf{drug D}}, \tag{12}$$

$$\epsilon_d\frac{\partial d}{\partial t} = \frac{\partial^2 d}{\partial x^2} + \Gamma b(1-d) - \underbrace{\frac{\beta_1\rho_5 n_1}{1+\rho_5 n_1}d}_{\textbf{drug A}} - \underbrace{\frac{\beta_2\rho_6 n_2}{1+\rho_6 n_2}d}_{\textbf{drug A}} - \underbrace{\beta_3 cd}_{\textbf{drug B}} - \underbrace{\frac{\beta_4\rho_5 n_3}{1+\rho_5 n_3}d}_{\textbf{drug C}} - \underbrace{\frac{\beta_5\rho_5 b}{1+\rho_5 b}d}_{\textbf{drug D}} - \lambda_3 d. \tag{13}$$

The corresponding boundary and initial conditions are

$$\frac{\partial n_2}{\partial x}(0,t) = 0, \qquad \frac{\partial a}{\partial x}(0,t) = -hb(1-a),$$

$$\frac{\partial c}{\partial x}(0,t) = p_1 bc, \qquad n_3(0,t) = e^{-kt}, \qquad \frac{\partial d}{\partial x}(0,t) = -\Gamma b(1-d), \tag{14}$$

$$\frac{\partial n_2}{\partial x}(1,t) = 0, \qquad \frac{\partial a}{\partial x}(1,t) = 0,$$

$$\frac{\partial c}{\partial x}(1,t) = 0, \qquad \frac{\partial n_3}{\partial x}(1,t) = 0, \qquad \frac{\partial d}{\partial x}(1,t) = 0, \tag{15}$$

$$n_1(x,0) = 1 - n_2(x,0), \qquad n_2(x,0) = \frac{1}{1+\exp(-\epsilon_2(x-a_2))}, \qquad a(x,0) = 1,$$

$$c(x,0) = 0, \qquad n_3(x,0) = \frac{1}{1+\exp(\epsilon_3(x-a_3))},$$

$$b(x,0) = \frac{1}{1+\exp(\epsilon_4(x-a_4))} \qquad d(x,0) = \frac{1}{1+\exp(\epsilon_5(x-a_5))}. \tag{16}$$

We note that in practice, at $t = 0$, the tumour may not yet have elicited angiogenic response or it may already be vascularized. The boundary and initial conditions we use are analogous to those from [28] and we assume that initially some tumour cells are situated at $x = 1$ awaiting angiogenesis. Experimental studies by Stokes and Lauffenburger [47] suggest that during angiogenesis there is a one-off formation of the capillary tips at $x = t = 0$. After this time capillary tips no longer originate from the limbus and instead they move away, so that the density at the limbus decreases. Based on these observations, and following [21], we impose the boundary condition $n_3(0,t) = e^{-kt}$, where k represents the rate of tip decrease at the limbus. Blood-borne removal of VEGF at the limbus is modelled by imposing a mixed boundary condition of the form $\frac{\partial c}{\partial x}(0,t) = p_1 bc$, where p_1 represents the rate of VEGF removal by the vessels at the limbus. The host vessels supply the region with oxygen and drug and therefore we have $\frac{\partial a}{\partial x}(0,t) = -hb(1-a)$ and $\frac{\partial d}{\partial x}(0,t) = -\Gamma b(1-d)$, where h and Γ represent the rates of oxygen and drug delivery by the limbal vessels. For
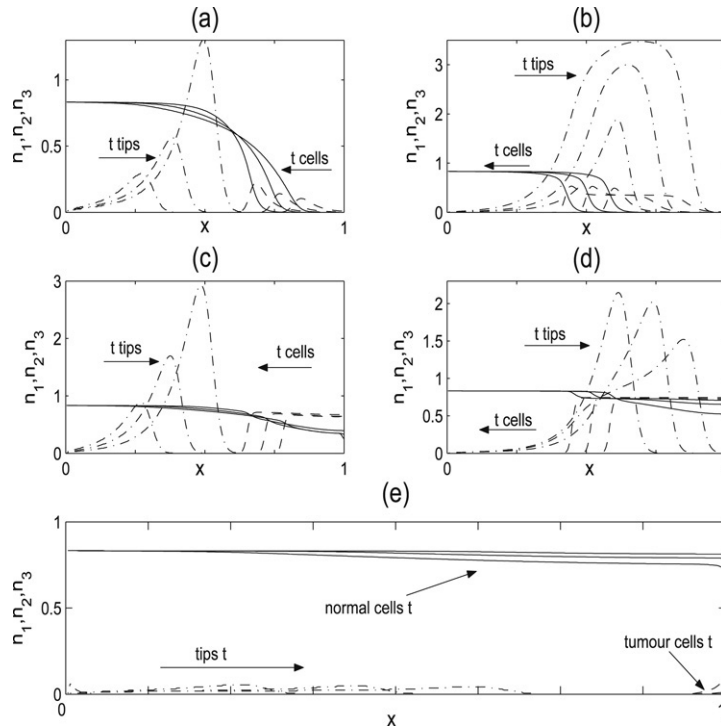
Fig. 1. Series of plots illustrating the types of behaviour that emerge from Eqs. (7)–(16) in the absence of therapy. The normal n_1 (−) and the tumour cell density n_2 (−−) propagate as waves of normal cell regression and tumour invasion, respectively, before and after successful vascularization (a)–(d); or when the normal cells are better competitors the tumour density regresses (e) in which case angiogenesis is unsuccessful. After successful vascularization the tumour grows larger ((b) and (d)). During angiogenesis in (a) and (c) the capillary tips n_3 (−.−) propagate from the limbus towards the tumour with increasing speed and increased maximum density. Post angiogenesis, tip profiles propagate with constant speed and either increase to a maximum value within the tumour mass (b) or decrease towards the tumour centre (d). The results are shown at dimensionless $t = 5, 10, 15$ in (a), (c) and (e) and $t = 20, 25$ and 30 in (b) and (d). Parameter values: $r_1 = 4, \rho_1 = 8, R_1 = 1, r_2 = 10, \rho_2 = 15,$ $R_2 = 2, d_{n_2} = 0.0007, h = 10, \lambda_1 = 0.1, r_3 = 0.1, r_4 = 10, p_1 = 10, d_c = 0.28, \gamma = 1, d_{n_3} = 0.0001, \psi = 0.8, \eta = 1.5, p_2 = 50, \beta_1 = 10,$ $s_1 = 1, \delta = 0.25, k = 30, p_3 = 10, \epsilon_d = 0.001, \Gamma = 0.1, \beta_i = 0, i = 1, \ldots, 5, \lambda_3 = 1, \epsilon_2 = 250, a_2 = 0.9, \epsilon_3 = \epsilon_4 = 250, a_3 = a_4 = 0,$ $a_5 = 0, \epsilon_5 = 500$ and (a) $c_1 = 10, c_2 = 5, \lambda_2 = 50$ in (b) $c_1 = 1, c_2 = 5, \lambda_2 = 0.5$ and in (c) $c_1 = 1, c_2 = 25, \lambda_2 = 50$.

the tumour density we impose a no-flux boundary condition so that $\frac{\partial n_2}{\partial x}(0, t) = 0$. Since we do not require boundary conditions for n_1 and b (see (7) and (12)), Eq. (14) complete our specifications at $x = 0$.

We assume symmetry of the tumour about its centre and hence impose no flux boundary conditions for n_2, a, c, n_3 and d at $x = 1$ (see Eq. (15)). As before we do not need to specify boundary conditions for n_1 (see (7)) and b (see (12)) at $x = 1$.

The initial profiles for n_1, n_2, a, n_3, b and d in (16) are chosen to be smooth functions that are consistent with the boundary conditions. We assume that initially some tumour cells are located at $x = 1$ and that the rest of the domain is filled with normal cells. Initially the vasculature is only present near the limbus, the region is well-oxygenated and there is no VEGF present.

3. Summary of results from [28]

Before we proceed with analysis of the system of equations (7)–(16) we present a brief summary of the results from [28] describing vascular tumour growth in absence of therapy.

Our results in [28] suggest that, in the absence of therapy, the tumour first undergoes a stage of initial avascular growth which is characterized by invasion of the host tissue. Following successful angiogenesis the tumour grows as a vascular tumour (see Fig. 1(a)–(e)). Vascular growth is characterized by a rapid increase in tumour density and increased speed of invasion. Furthermore our model predicts that tumour–host interactions control vascular tumour growth. Recalling that c_1 and c_2 represent the adverse effect of the tumour cells on the normal cells and vice versa, we
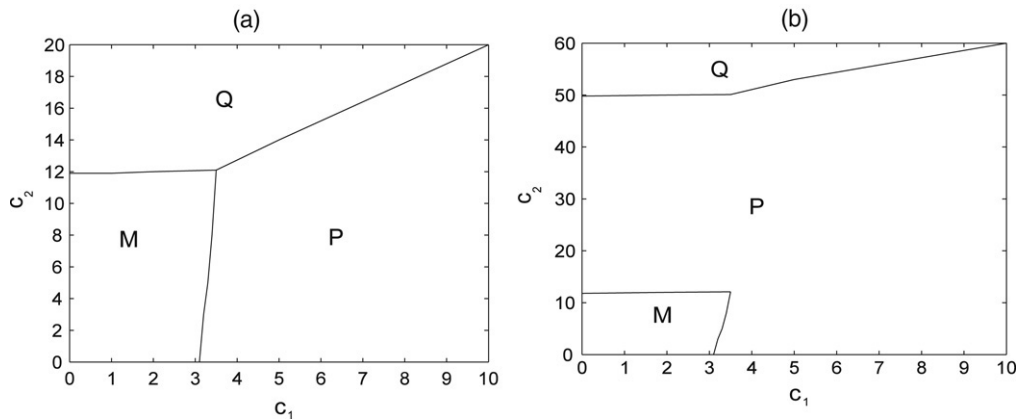
Fig. 2. (a) Diagram showing how the competition parameter space (c_1, c_2) can be decomposed into distinct regions depending on the long time behaviour of the model solutions, for two different values of λ_2 before any therapy. In (a) $\lambda_2 = 5$ and in (b) $\lambda_2 = 50$ with the rest of the parameters as per Fig. 1. Three outcomes are evident: the tumour and host cells coexist in region M, tumour cells dominate in region P and the tumour is cleared by the host cells in region Q.

predict that before chemotherapy the (c_1, c_2) parameter space contains distinct regions M, P and Q where tumour–host interactions result in different long term solutions (see Fig. 2(a) and (b)). In region P the tumour eventually dominates and replaces the normal cells; in region Q the normal cells dominate and replace the tumour cells; in region M the tumour coexists with the normal cells. The bifurcation curves that divide these regions depend on λ_2, a parameter which represents the rate at which oxygen is consumed by the tumour cells (see Eq. (9)).

In the next five sections we explore how the vascular tumour growth dynamics described above changes in the presence of three different treatment strategies used in isolation or in combination. We compare tumour growth to that in [28].

4. Therapy targets proliferating cells (drug A)

In this section we use Eqs. (7)–(16) to study the effect of a drug that targets the proliferating cells. We assume that drug A is delivered to the vascular tumour by the vasculature and that it does not target VEGF or the vasculature. Accordingly we fix $\Delta_3 = \Delta_4 = \Delta_5 = 0$ and $\beta_3 = \beta_4 = \beta_5 = 0$ in Eqs. (7)–(16).

We use the NAG library routine DO3PCF to perform our numerical simulations. This routine discretizes the equations using finite differences and solves the resulting system of ordinary differential equations using backward differentiation [48]. We find that, depending on the parameter values, the system admits 3 qualitatively different types of behaviour: the tumour undergoes vascular growth (i.e. chemotherapy with drug A is ineffective and profiles are as per Fig. 3(a)); the tumour experiences arrested growth with the tumour mass reaching a finite size (limited success of the drug A and profiles as per Fig. 3(b)) or it is eliminated (successful treatment with drug A and profiles as per Fig. 3(c)).

The key (dimensionless) parameters associated with incorporating different tumour types in our model are c_1, c_2, λ_2, r_4, Δ_1, Δ_2 and β_2. The parameters associated with drug A are Δ_1, Δ_2, β_1, β_2, D_d, Γ and λ_3. Where possible we use published data for the treatment of nude mice with the anti-cancer drug doxorubicin that targets proliferating cells. In Table 2 we list these parameters, their dimensional and dimensionless values and the source of the parameter estimates. Experimental studies involving doxorubicin [49,51] suggest that it induces apoptosis in tumour and healthy cells but that normal tissue is more resistant to therapy because its uptake is about a tenth that of the tumour cells [49]. Motivated by this we assume that (dimensionless) $\beta_1 \ll \beta_2$.

We use results from [28] to fix the other model parameters so that in the absence of therapy the tumour becomes vascularized after 14 days. Upon vascularization chemotherapy with drug A is initiated. The different outcomes presented in Fig. 3(a)–(c) can be obtained from our mathematical model by varying the parameters Δ_1, Δ_2 and β_2. We explore $(\Delta_1, \Delta_2, \beta_2)$ parameter space and present our results in Fig. 4(a) and (b). We constructed Fig. 4(a) and (b) by solving the Eqs. (7)–(16) numerically for different values for Δ_1, Δ_2 and β_2 to determine the bifurcation curves that represent the transitions between different regions.
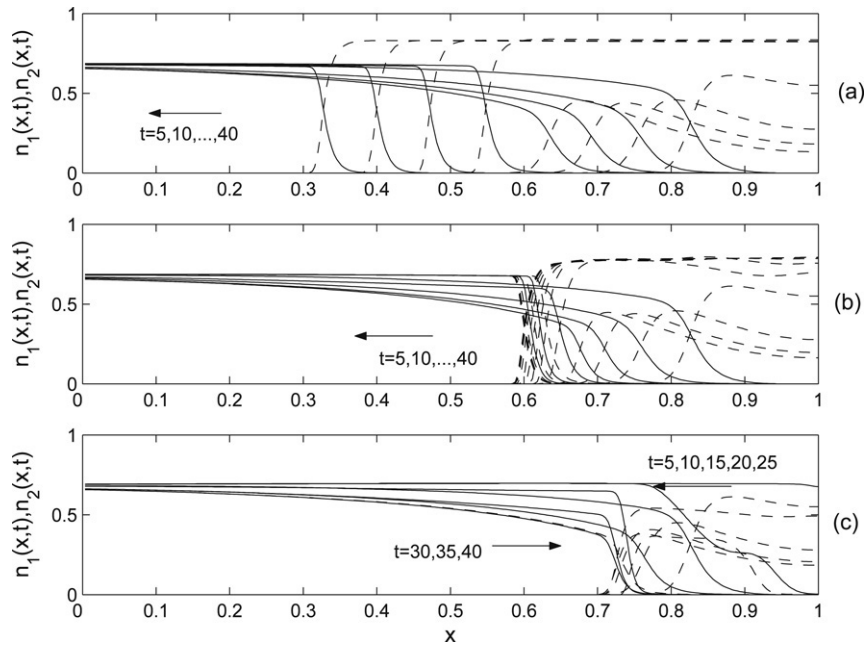
Fig. 3. Series of plots illustrating the types of behaviour that emerge from Eqs. (7)–(16) under the influence of anti-proliferative therapy. We change the parameters that control the therapy effectiveness Δ_2, β_2 and the rest of the parameters are fixed as per Fig. 1(a)–(e). The profiles of the normal cell density are denoted by $n_1(x, t) = -$ and the tumour cell density by $n_2(x,) = --$. (a) When $(\Delta_2 = 1, \beta_2 = 1) \in N$ in Fig. 4(b) the therapy fails and the tumour proceeds to grow and invade the host tissue. The profiles propagate towards the left and resemble those in Fig. 1(a) and (b). (b) When $(\Delta_2 = 10, \beta_2 = 0.5) \in S$ in Fig. 4(b) the therapy is partially effective and as a result the vascular tumour is growth-arrested at time $t = 40$. After this time the tumour stays at this growth-arrested size. (c) When $(\Delta_2 = 25, \beta_2 = 3) \in R$ in Fig. 4(b) chemotherapy with a type A drug is successful. Prior to therapy ($t = 5, 10, \ldots, 25$) the tumour grows and invades with its profiles propagating towards the left into the host tissue. As a result of the therapy after $t = 25$ tumour invasion is reversed and the tumour profiles regress towards the right, until the tumour is eventually removed. The region is filled with host cells only in the long time.

Table 2
Parameter estimates for drug A (doxorubicin)

Dimensional parameters		Dimensionless parameters		
Parameter	Estimate	Parameter	Magnitude	Reference
D_d	1.7 cm^2 day^{-1}	n/a	1	Dordel et al. [51]
λ_3	1.9 day^{-1}	$\lambda_3^* = \lambda_3 \frac{L^2}{D_d}$	$[O(1), O(10)]$	Baxter et al. [31]
Δ_1	56 M^{-1} day^{-1}	$\Delta_1^* = \Delta_1 \frac{T D_{\text{vess}}}{K_1}$	$O(1)$	Dordal et al. [51]
Δ_2	560 M^{-1} day^{-1}	$\Delta_2^* = \Delta_2 \frac{T D_{\text{vess}}}{K_2}$	$O(10)$	Dordal et al. [51]
β_1	No available data	$\beta_1^* = \beta_1 \frac{L^2}{D_d}$	Modelling assumption	
β_2	2 day^{-1}	$\beta_2^* = \beta_2 \frac{L^2}{D_d}$	$[O(10^{-1}), O(10)]$	Baxter et al. [31]

We find that the (Δ_1, Δ_2) parameter space partitions into four distinct regions I–IV depending on whether the density of the tumour and the normal cells are reduced when drug A is present. In region I neither the tumour cell nor the normal cell density is reduced and the vascular tumour growth proceeds as if no drug was applied (see Fig. 4(a)). When (Δ_1, Δ_2) lie in region II the waves of tumour invasion that were present prior to chemotherapy are replaced either by waves of tumour regression or tumour invasion is halted and the normal cell density is not reduced (profiles are similar to those in Fig. 3(b) and (c)). In this case chemotherapy effectively controls tumour invasion and arrests vascular tumour growth. When (Δ_1, Δ_2) lie in regions III or IV (see Fig. 4(a)), then either both the tumour and the normal cell densities are reduced or only the normal cell density is reduced. In the latter case the chemotherapy is not strong enough to kill the tumour cells (Δ_2 is below the threshold) and this case corresponds to the pathological case of
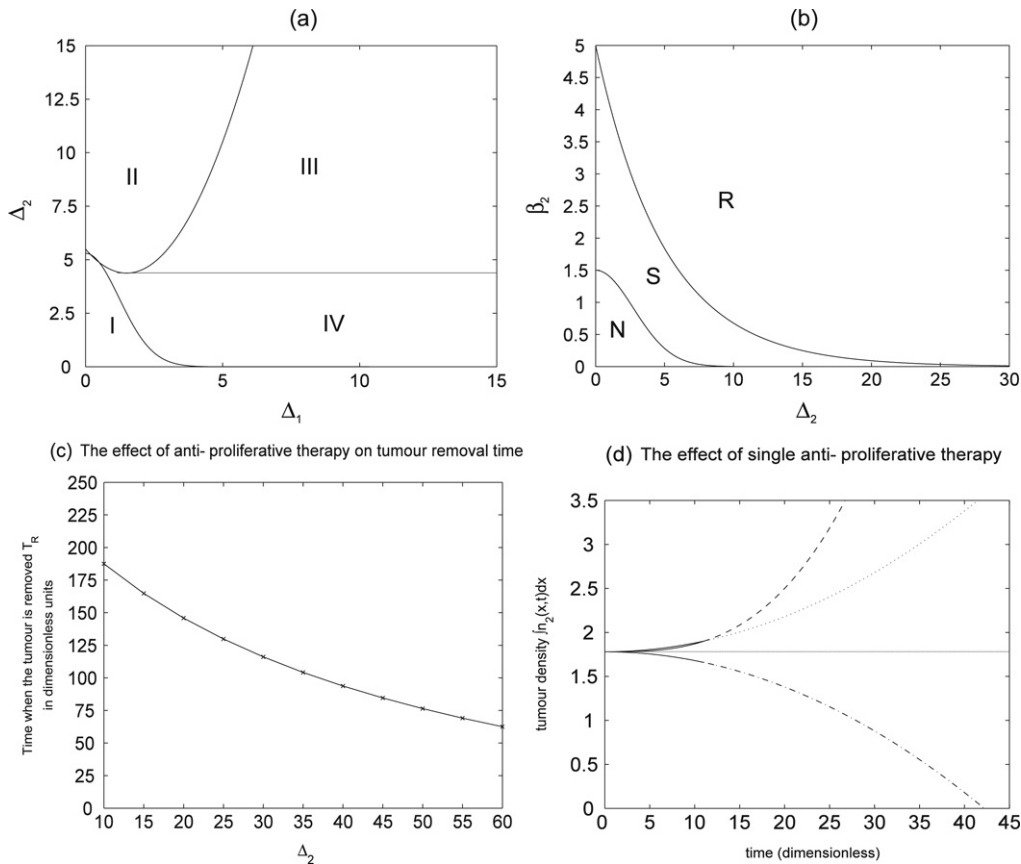
Fig. 4. (a) and (b) Diagrams illustrating how the (Δ_1, Δ_2) and (Δ_2, β_2) parameter spaces can be decomposed into distinct regions depending on the long-term behaviour of the tumour and the healthy cells. (a) In the long term, only tumour cells are killed (II), only normal cells are killed (IV), both cell types are killed (III), or there is no effect on tumour growth (I). Qualitatively the structure of the (Δ_1, Δ_2) parameter space is independent of β_2 provided that $c_1 \geq c_2$ to allow for tumour vascularization. (b) The therapy is not effective in region N; the tumour regresses and is removed in region R and the tumour is growth-arrested in region S. The rest of the parameters are fixed as per Fig. 1(a) and (b) so that in the absence of therapy tumour cells dominate and invade the healthy tissue. (c) Numerically calculated decrease in the time to tumour clearance as a function of the potency of drug A on the tumour cells (Δ_2). We observe that as Δ_2 increases the tumour is cleared quicker. (d) Numerically calculated increase in total number of tumour cells $\int n_2(x, t)\mathrm{d}x$ over time during vascular growth in absence of therapy $(--)$, during avascular growth in absence of therapy (...) and for two different therapy outcomes. In one case the therapy removes the tumour $(-.-)$ so the total density decreases to zero, whilst in the other case tumour growth saturates $(-)$. In the former case we fix $\Delta_1 = 0.1$, $\Delta_2 = 10$ and $\beta_2 = 0.5$ and in the latter case $\Delta_1 = 0.1$, $\Delta_2 = 25$, $\beta_2 = 2$. The rest of the parameters are as per Fig. 1(a) and (b) and we calculate the values numerically. Avascular growth is calculated when we fix $\Delta_1 = \Delta_2 = \beta_2 = 0$ and $\psi = 1$, $\eta = 10$ with the rest of the parameters as per Fig. 1(a) and (b).

a tumour growing in a dead host. We consider this case as biologically irrelevant. The former case corresponds to death of the tumour and the host with the normal cell density reaching to zero before the tumour is cleared. Hence our simulations suggest that an antiproliferative drug is effective only when $\Delta_1 \ll \Delta_2$ (region II of Fig. 4(a)). The biological interpretation of our results is drug A will be successful in controlling tumour growth only if it has negligible impact on the normal cells, and high potency on the tumour cells. These results are consistent with experimental observations. For example in [49] doxorubicin was shown to be effective in human Ewing's carcinoma if its toxicity to tumour cells was large and its toxicity to healthy tissue was negligible. As Δ_2, i.e. the potency of the drug A on the tumour cells, increases in region II, the tumour is cleared more quickly and thus the therapy is more effective (see Fig. 4(c)).

Our simulations show that the response to drug A also depends on the dimensionless parameter β_2 that characterizes the drug's uptake by the tumour cells (see Eq. (13)). Keeping the rest of the parameters fixed so that prior to therapy the tumour dominates the healthy cells, vascularizes and invades the adjacent tissue, in Fig. 4(b) we decompose the (Δ_2, β_2) parameter space into distinct regions based on the predicted therapeutic outcome. The diagram shows that either the therapy is not effective in controlling vascular invasion (region N), tumour invasion of the host tissue is

reversed and the tumour regresses (region R), or tumour invasion of the host tissue is halted and the tumour undergoes saturated growth (region S). When β_2 and Δ_2 are small we predict that the therapy is ineffective: proliferation of the tumour and normal cells is unaffected by the drug and so the tumour continues to grow and invade. As β_2 and Δ_2 increase, corresponding respectively to an increase in the rate at which the tumour cells uptake the drug, or an increase in its potency, the rate of cell death increases, tumour invasion is reversed and the tumour eventually eliminated (in region R of Fig. 4(b)). These results are consistent with *in vivo* observations [49] showing an increase in the rate of tumour cell death and possible tumour clearance when the rate at which tumour cells uptake the drug doxorubicin and/or its potency are increased. These results are also consistent with theoretical predictions concerning doxorubicin that were developed by Jackson [50]. In contrast to [50] our results suggest the existence of a region (region S) in which the tumour undergoes saturated growth and does not regress. Saturated growth in previous mathematical models (e.g. Ward and King [17]) is a consequence of the degradation of the necrotic material in the tumour centre. Unless this occurs there is no saturated tumour growth. However, to the best of our knowledge arrested growth has not been captured in previous mathematical models for anti-proliferative therapies, although it has been observed *in vivo* tumours [49,51].

The response to the simulated anti-proliferative chemotherapy depends markedly on the competitive effects of the tumour cells on the normal cells (c_1) and vice versa (c_2). Next we investigate how the distinct regions M, P and Q of the (c_1, c_2) parameter space (see Fig. 2(a) and (b)) change upon application of therapy. When the therapy is of limited success ((Δ_2, β_2) $\in S$ in Fig. 4(b)) our results suggest a change in the long time solutions characterized by the shifts: $M \rightarrow Q$ so that the region where tumour–host coexistence was present before therapy is replaced by a region where the tumour is cleared following treatment with drug A; and a shift $P \rightarrow M$ so that the region of tumour dominance and invasion before therapy is replaced by a region in which invasion is controlled and the tumour is growth arrested following treatment with drug A. When the therapy is successful ((Δ_2, β_2) $\in R$ in Fig. 4(b)) the tumour is cleared for any values of the competition parameters c_1 and c_2 and in the respective Fig. 2(a) and (b) the following shifts are evident: $M \rightarrow Q$ and $P \rightarrow Q$. These results suggest that drug A applied to a tumour that dominates the host tissue will clear the tumour if its potency and uptake by the tumour cells are large ((Δ_2, β_2) $\in R$ in Fig. 4(b)). When drug A is applied to a tumour that coexists with the host cells, we predict that neither its potency on the tumour cells nor its uptake need be large for the therapy to successfully remove the tumour. In this case for values (Δ_2, β_2) $\in S$ or R in Fig. 4(a) and (b) the longtime solutions are characterized by the shifts $M \rightarrow Q$ and $P \rightarrow Q$ in the (c_1, c_2) parameter space in Fig. 2(a) and (b). Therefore in the longtime the region of tumour dominance or tumour–host coexistence is replaced by a region where healthy host cells dominate. These results allow us to predict that success of treatment with drug A depends on the drug's potency and its rate of uptake by the tumour cells, as well as the composition of the tissue in the tumour surrounding.

We note that in our results the success of treatment with drug A does not depend on the rate of drug's uptake by the normal cells. From Table 2 and also in results from [52], the uptake by the normal cells is an order of magnitude less than that by the tumour cells. Thus in our simulations, the uptake by the normal cells was O(1) and its increase dis not alter the results.

Our simulations also suggest that when (c_1, c_2) $\in Q$ in Fig. 2(a) and (b) so that before therapy the host tissue is a better competitor and dominates the tumour cells, the tumour will be cleared regardless of the strength of the therapy (region Q does not change when drug A is administered).

We also run simulations where at one point the therapy with drug A is switched off and then switched on again (by decreasing or increasing β_2 and Δ_2 below or above their thresholds in Fig. 4(b) as appropriate after a few timesteps). Our results predict that in such a case the longtime behaviour of the tumour resembles tumour growth in absence of therapy studied in [28]. The longtime solutions of the tumour and host cell density depend on the competition parameters c_1 and c_2 and two qualitative outcomes are evident: either the tumour undergoes vascularization and grows as a vascular tumour either replacing the healthy cells ((c_1, c_2) $\in P$ in Fig. 2(a) and (b)) or coexisting with them ((c_1, c_2) $\in M$ in Fig. 2(a) and (b)); or the tumour is cleared by the healthy cells ((c_1, c_2) $\in Q$ in Fig. 2(a) and (b)). These results predict that continuous infusion with antiproliferative drug A is required to control vascular tumour growth.

5. Therapy targets VEGF (drug B)

In this section we use the Eqs. (7)–(16) to study the effect of a drug that targets the angiogenic stimulant VEGF. We assume that drug B is delivered to the vascular tumour by the vasculature and that it does not target proliferating

cells or the vasculature. Accordingly we fix $\Delta_1 = \Delta_2 = \Delta_4 = \Delta_5 = 0$ and $\beta_1 = \beta_2 = \beta_4 = \beta_5 = 0$ in Eqs. (7)–(16) so that the drug only has antiVEGF properties.

Numerical simulations suggest that continuous infusion with a drug of type B gives rise to two qualitatively different outcomes: either the drug is ineffective and the tumour continues to undergo vascular growth or it is successful, the vasculature is eliminated and the tumour undergoes avascular growth. Qualitatively speaking, tumour invasion of the healthy cells is unaltered by this therapy but the speed of invasion is reduced, being similar to that prior to tumour vascularization. As a result the tumour grows more slowly than in the absence of therapy. The key parameters that control whether this therapy succeeds (and makes the tumour resume avascular growth) are Δ_3, its potency on the tumour cells, and r_4, the (maximum) rate of VEGF secretion by the tumour.

Following effective antiVEGF therapy the tumour profiles are similar to the profiles depicted in Fig. 1(a), and represent avascular growth with decreased cell density behind the leading tumour front. This resembles the growth of multicellular spheroids *in vitro* [2] where the tumour cell density decreases from the outer edge of the tumour towards the centre. We recall that our results in [28] suggest that in the absence of therapy the tumour grows as an avascular tumour if tip chemotaxis towards VEGF is weak. Therefore the effect of antiVEGF therapy is the same as if tip chemotaxis is sufficiently reduced: in both cases the tumour undergoes avascular growth only.

In Fig. 5(a) we show how the (Δ_3, r_4) parameter space splits into two regions depending on the long term model solutions. Either the tumour evolves to a large and invasive vascular tumour (ineffective therapy in region V_2 of Fig. 5(a)) or (under effective therapy in region V_1 of Fig. 5(a)) there is a reduction in its vascular density and the corresponding vascular profiles differ from those during successful angiogenesis (compare Fig. 6(a) and (b) with Fig. 6(c) and (d)). The tumour grows slower following antiVEGF therapy (see Fig. 5(b)) in agreement with the results from [26].

Our simulations suggest that under hypoxia (induced by large consumption of oxygen i.e. large λ_2) the therapy fails if too much VEGF is produced by the hypoxic tumour cells i.e. when r_4 is above a certain threshold, regardless of the size of Δ_3. This agrees with clinical studies in which the drug Thrombospondin was used as an antiVEGF drug [53]. This therapy was effective under hypoxia only when low levels of VEGF were secreted regardless of the amount of the antiVEGF drug Thrombospondin administered [53].

Although antiVEGF therapy can transform a vascular tumour into its avascular counterpart, it cannot prevent tumour invasion. Our simulations suggest that tumour invasion is independent of the success of the antiVEGF therapy and is controlled instead by the strength of tumour–host competition (by the parameters c_1 and c_2). The qualitative form of the (c_1, c_2) parameter space resembles that in Fig. 2(a) and (b) with three distinct regions evident. In these regions either (i) the tumour cells dominate and replace the normal cells (region P); (ii) the normal cells dominate and replace the tumour cells (region Q); or (iii) the tumour and host cells coexist (region M).

We also run simulations where at one point the antiVEGF therapy is switched off (by decreasing Δ_3 below its threshold as in Fig. 5(a) after a few timesteps) and then switched on again. Our results predict that in such a case the tumour will become vascularized in the long time although the time for tips to reach the tumour is slightly longer. In particular, when we keep Δ_3 large for the first five dimensionless timesteps and then decrease it to zero, the time of tumour tip-contact is approximately 21 (dimensional) days after the initial time. Therefore having the anti-VEGF therapy effective initially has lengthened the vascularization time compared to 15 days in Fig. 1(a)–(d) if no therapy was initially present. The longtime profiles resemble those in Fig. 1(b) or 1(c) depending on the choice for c_1 and c_2. If the therapy is initially on for five timesteps, then is switched off for five timesteps and then switched on again, qualitatively the results represent unsuccessful antiVEGF therapy. In the long time the tumour remains vascular and does nor revert to avascular growth. These results predict that when the antiVEGF therapy is not being administered continuously the tumour becomes vascularized. Once antiVEGF therapy is switched off the tumour initiates and completes angiogenesis rapidly, and even though we then increase Δ_3 so $(\Delta_3, r_4) \in V_1$ in Fig. 5(a), the tumour does not revert to an avascular mass. Instead it grows as an invasive vascular tumour. Therefore our model predicts that discontinuous antiVEGF therapy is not effective anticancer treatment. This result is expected since although antiVEGF therapy will reduce the VEGF influence in the region preventing further angiogenesis, it will not affect the neovasculature formed in the time when the antiVEGF therapy is switched off.

6. Therapy targets the tumour vasculature (drug C or drug D)

An alternative to antiproliferative or antiVEGF therapy involves targeting the tumour vasculature with antivascular
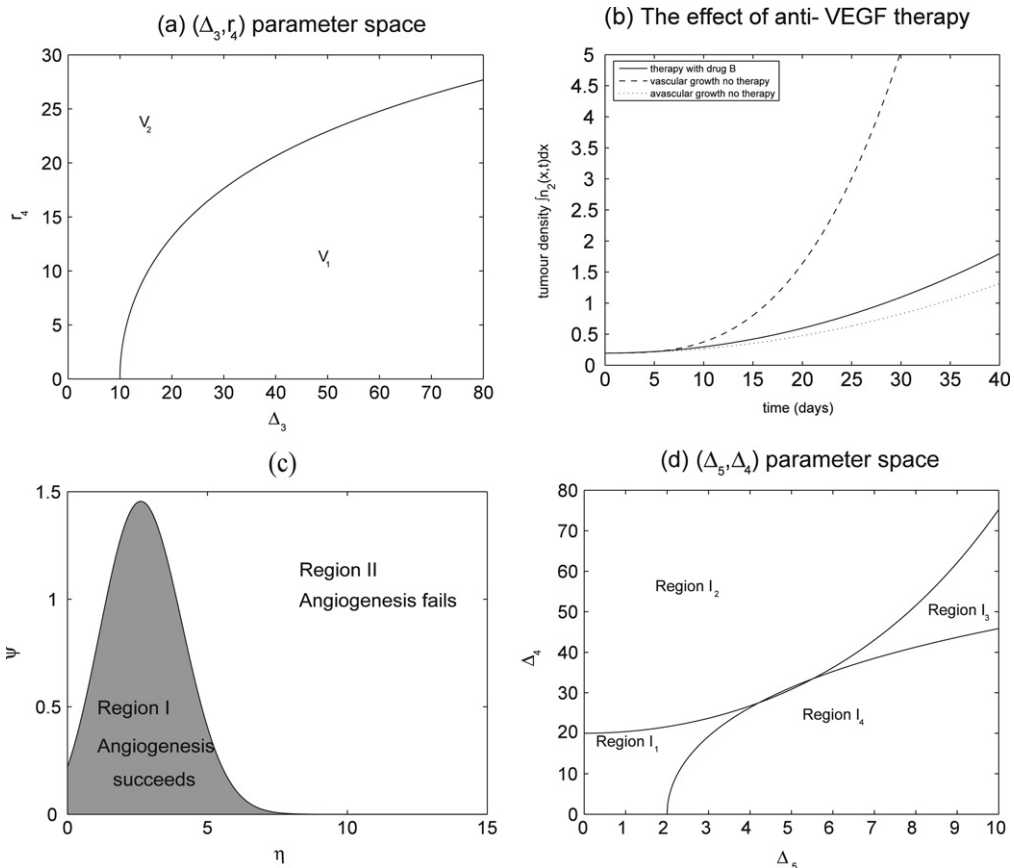
Fig. 5. (a) Diagram illustrating how the (Δ_3, r_4) parameter space can be decomposed into distinct regions depending on the long time behaviour of the model solutions. The different regions are determined depending on the solutions following antiVEGF therapy. The therapy is effective in reverting a vascular tumour to avascular and preventing further angiogenesis in region V_1 and is not effective in region V_2. (b) Numerically calculated rate of tumour growth following antiVEGF therapy and comparison with the rate of growth in absence of therapy during avascular and vascular growth. (c) Diagram showing the existence of a numerically calculated region where the tumour grows as avascular or vascular depending on the values of the chemotactic parameters η and ψ. This parameter space is determined by detailed numerical simulation. The rest of the parameter values are as per Fig. 1(a) with the tumour being the better competitor and $(c_1, c_2) \in P$ from Fig. 2(a) and (b). Qualitatively the results are the same when $(c_1, c_2) \in M$ from Fig. 2(a) and (b). (d) Diagram illustrating how the (Δ_5, Δ_4) parameter spaces can be decomposed into distinct regions depending on the long time behaviour of the model solutions. The regions are determined depending on whether in the long term the vascular content in the region is destroyed and the tumour grows avascularly (regions I_3 and I_4), only the angiogenic capillary density is reduced (region I_2), or the therapy has no impact and the tumour grows as a vascular tumour (region I_1).

drugs such as cyclophosphomide [12] or combretastatin CAP4 [35]. In this section we use Eqs. (7)–(16) to study the effect of drugs with such anti-vascular properties. We distinguish between anti-vascular drugs that target the (immature) capillary tips and those that destroy the (mature) blood vessels in the peritumoural environment. Accordingly we assume that drugs C or D are delivered to the vascular tumour by the vasculature, that they do not affect the proliferating cells or the VEGF and we investigate the impact on the tumour's growth dynamics of continuous infusion with such drugs. To focus on drugs that target only the vasculature we set $\beta_1 = \beta_2 = \beta_3 = \Delta_1 = \Delta_2 = \Delta_3 = 0$ and assume that $\Delta_4, \Delta_5 > 0$.

In the absence of suitable experimental data, we assume that the diffusion coefficient and the delivery rate of the antivascular drugs are similar to those of an anti-proliferative drug. Accordingly we fix D_d and Γ at levels similar to those used in Section 4.

Following their successful delivery, the potency of drugs C or D dictates whether they reduce the density of the angiogenic capillaries only or reduce the density of all tumour blood vessels.

When drug C is employed tumour dynamics are controlled by the balance between its potency (Δ_4) and the rate at which vessels produce tips (p_2). Effective therapy with drug C reduces the density of the angiogenic tips only, and
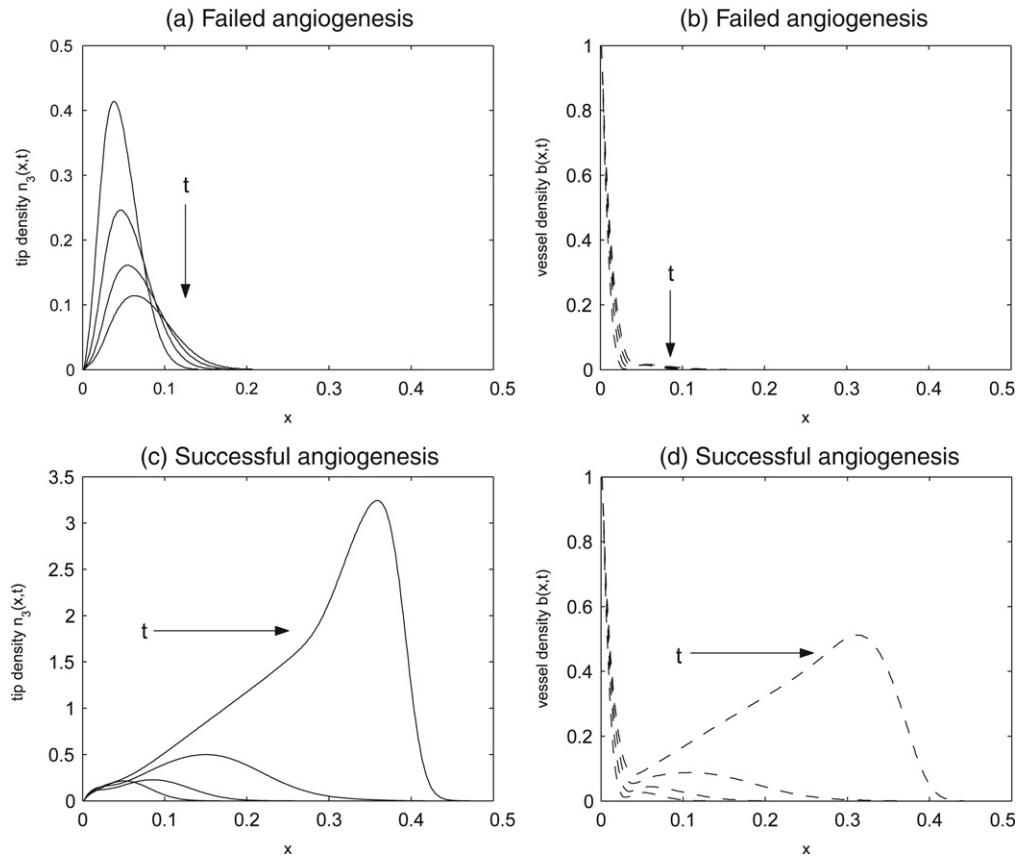
Fig. 6. Series of plots illustrating the profiles of the capillary tips and the vessel density during unsuccessful angiogenesis (a) and (b) and during successful angiogenesis with brush border (c) and (d). The parameters are as in Fig. 1(a) apart from $\gamma = 19, \eta = 50$ for (a) and (b) and $\gamma = 1, \eta = 1.5$ for (c) and (d). We plot the profiles at dimensionless $t = 5, \ldots, 20$.

in so doing slows tumour growth rate. We note that the vessel density is slightly reduced but blood vessels persist in the peritumoural environment. Spatial gradients of VEGF mean that tumour vascularization is ongoing but angiogenic tips are destroyed with drug C. The reduction in tip density is most dramatic when $\Delta_4 \gg p_2$ and the drug's potency is much greater than the rate of tip production. In this case existing tips are killed more rapidly than new ones can be produced. Consequently the treated tumour grows more slowly than its untreated counterpart (see Fig. 7(a)). Finally, we remark that the dynamics of the tumour–host interactions are unchanged following treatment with drug C. As a result the (c_1, c_2) parameter space has the same qualitative decomposition as in Fig. 2(a) and (b) (results for drug C not shown).

When drug D is delivered to the tumour its overall growth rate is retarded when drug potency on the blood vessels (Δ_5) is large (see Fig. 7(a)). In this case the host blood vessels are destroyed and no new tips can be produced. Angiogenic tips that have reached the tumour prior to therapy will not be destroyed, so while some neovasculature may occur at the tumour site, further angiogenesis is prevented. However since the blood vessels in the peritumoural environment deliver oxygen as well as drugs, their destruction makes the region hypoxic. This affects the growth dynamics and in our simulations is manifested by a decrease in the overall density of the healthy tissue. This is an undesirable outcome and suggests that treatment with drug D may have a strongly deleterious effect on the normal tissue. Although our simulations show that normal and tumour cell densities are reduced following such treatment, the dynamics of the tumour–host interactions remain unaltered. In particular, if the tumour (or the normal) cells dominate prior to therapy they will continue to do so following therapy. Equally if tumour–host coexistence is present before treatment it will persist after therapy. Therefore the (c_1, c_2) parameter space is similar to that presented in Fig. 2(a) and (b).

Next we compare the effects of drugs C and D. In our simulations targeting the angiogenic vasculature (drug C)
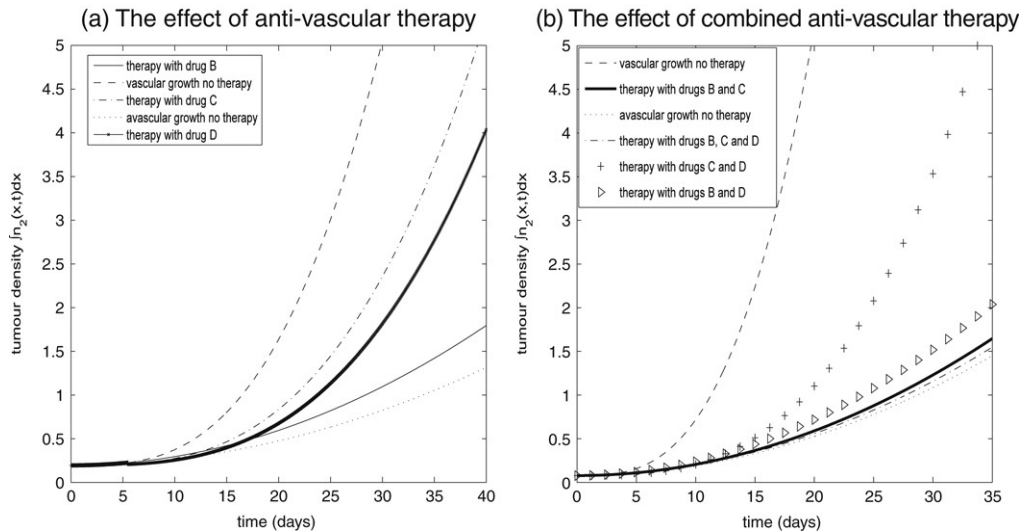
Fig. 7. (a) and (b) Numerically calculated increase in the total number of tumour cells calculated as $\int n_2(x, t)\mathrm{d}x$ from our simulations. We plot this value at different times. We contrast the rate of increase when the tumour only completes the avascular growth phase to that when it can become vascularized, as well as to the rate of growth in presence of single (a) and combined (b) antivascular therapies. These results are obtained when we solve (7)–(16) for parameter values depending on which therapy is effective.

results in a vascular tumour with a small density of angiogenic vessels and large density of host blood vessels. In contrast, targeting the blood vessels (drug D) will diminish the vessel density of the vascular tumour whilst some angiogenic capillaries will persist at the tumour site. In Fig. 7(a) we observe that following treatment with drugs C or D reduces the overall growth of the tumour mass. These growth curves lie between those for an untreated vascular tumour and an untreated avascular tumour. The tumour grows more rapidly when drug C is applied (see Fig. 7(a)).

As mentioned previously, the potency of drugs C and D (Δ_4 and Δ_5) are key parameters that control their efficacy in our simulations. In Fig. 5(d) we decompose the (Δ_4, Δ_5) parameter space into distinct regions depending on the long time vascular content. Four distinct regions are observed. In region I_1 the therapy has no impact and the tumour retains a large vascular component of both blood vessels and angiogenic tips. In region I_2 drug C is effective and the impact of drug D is negligible. Hence only angiogenic vasculature is destroyed. Similarly in region I_4 drug D is effective and drug C is not. In this region blood vessels are destroyed, but any tips that reached the tumour before therapy will not be destroyed. Finally in region I_3 both drugs C and D are effective: the angiogenic tips and the blood vessels are destroyed, reducing the overall vascular content to zero. The tumour growth rate reduces to that for avascular growth (see Fig. 7(a) and (b)). Therefore we predict that antivascular therapy will cause a vascular tumour to revert to an avascular form only when it destroys both the angiogenic tips and the blood vessels. We note, however, that for the potency rates in region I_4 of Fig. 5(d), the healthy cell density is reduced. As mentioned previously, this is a consequence of the hypoxia that occurs when the oxygen-bearing host blood vessels are destroyed.

As for antiVEGF therapy, in our model successful antivascular therapy can transform a vascular tumour to its avascular counterpart, but cannot prevent tumour invasion. The qualitative form of (c_1, c_2) parameter space resembles that in Fig. 2(a) and (b): the tumour cells dominate and replace the normal cells (region P); the normal cells dominate and replace the tumour cells (region Q); or the tumour and host cells coexist (region M).

We also run numerical simulations where anti-vascular therapy is switched off after a few time steps and then switched on again (by first decreasing and then increasing Δ_4 and Δ_5 below and above the thresholds so they belong to regions I_1 and I_3 in Fig. 5(d)). Our results suggest that the tumour will become vascularized in the long time but the time of tumour-tip contact is greater the longer we keep the antivascular therapy switched on. In particular, keeping the potency rates large, and therapy effective, in the first five timesteps and then decreasing them to zero, so therapy is ineffective, increases the vascularization time from 15 (dimensional) days in absence of any initial therapy to 23 days. The profiles resemble those in Fig. 1(b) and (c) depending on the choices of competition parameters c_1 and c_2. Therefore we predict that continuous infusion with antivascular drugs C and D is required to control vascular tumour growth.

7. Combined antiVEGF and antivascular therapy (drug B, drug C and/or drug D)

Thus far we have studied the response of a vascular tumour to continuous infusion with antiproliferative, antiVEGF or anti-vascular drugs. Our results suggest that the antiproliferative therapy (drug A) is most effective in controlling vascular tumour growth since it can either reverse tumour invasion and clear the tumour or arrest its progression (see Fig. 3(c) and (b) respectively). In contrast, delivery of drug B, or a combination of drugs C and D reduces the overall tumour growth but does not control tumour invasion.

In this section we investigate the effect of infusing the vascular tumour with a combination of drugs B, C and D and, in so doing, study the impact of combined antiVEGF and antivascular therapies. To focus on therapy that targets the VEGF stimulant and the vasculature we set $\beta_1 = \beta_2 = \Delta_1 = \Delta_2 = 0$ and vary Δ_3, Δ_4 and/or Δ_5 respectively.

Our numerical simulations suggest two qualitatively different outcomes: either the tumour reverts to avascular growth (successful combined therapy) or it continues to undergo vascular growth (ineffective combined therapy). In particular the outcome is the same as that for effective treatment with drug B, or a combination of drugs C and D. Further tumour invasion is not altered when these therapies are applied.

When the tumour resumes avascular growth the vascular density is reduced and tumour growth rate retarded. Our simulations predict that this situation rises in the following cases:

1. When the angiogenic capillaries are destroyed (drug C) and the influence of the VEGF is reduced (drug B);
2. When the blood vessels surrounding the tumour are destroyed (drug D) and the influence of the VEGF is reduced (drug B);
3. When the blood vessels as well as the angiogenic tips around the tumour are destroyed (drugs D and C) in parallel to reduced influence of the VEGF stimulant (drug B).

Combinations of antiVEGF and antivascular therapy are effective if the potency of the drugs is large. The tumour's growth rate following treatment with combinations of drugs B, C and/or D differs from that when drug B is given in isolation and/or when drugs C and D are administrated. As Fig. 7(b) shows, the presence of an antiVEGF drug in combination with antivascular drugs C or D, slows down tumour growth. We undertake parameter sensitivity analysis and we calculate the increase in tumour growth under different combinations of drugs B, C and D. Our results predict that the increase in tumour mass ($\int n_2(x, t)dx$) is slowest when drugs B, C and D are combined. In contrast when drugs C and D only are combined the growth retardation is least i.e. this combination of antiVEGF and antivascular drugs is least effective. We label with $g(\Omega) = [\int n_2(x, t)dx]_\Omega$ the increase in the tumour mass under the influence of the therapy Ω[1] as plotted in Fig. 7(a) and (b). The results from Fig. 7(a) and (b) can be summarized as follows:

$$g(\Omega_0) < g(B) < g(D) < g(C) < g(\Omega_\infty) \tag{17}$$

$$g(\Omega_0) < g(BCD) < g(BC) < g(BD) < g(CD) < g(\Omega_\infty). \tag{18}$$

Therefore we predict that a combination of antiVEGF and antivascular drugs that destroy all the vasculature is most effective in reducing the increase in tumour mass. In comparison to when only antivascular therapy (combined drugs C and D) is effective, combined antiVEGF and antivascular therapy dramatically reduces tumour growth (see Fig. 7(b)) to that of avascular tumour in absence of therapy. We also remark that when drug B is combined with drugs C and/or D the increase in the tumour mass is slower than under isolated therapy with drugs B, C or D (comparing Fig. 7(a) and (b)).

8. Combined antiproliferative, antiVEGF and antivascular therapy (drug A and drugs B, C and/or D)

Thus far we have studied the response of a vascular tumour to continuous infusion with antiproliferative, antiVEGF, antivascular drugs or a combination of antiVEGF and antivascular drugs. In this section we use the Eqs. (7)–(16) to study the effect of a chemotherapy that simultaneously targets the proliferating cells, reduces the VEGF influence and destroys the tumour vasculature during vascular tumour growth. We assume that drugs A, B, C and D are delivered to the vascular tumour and vary their respective potency on the normal and tumour cells, VEGF and the vasculature

---

[1] We note that $g(\Omega_0)$ represents the increase in tumour mass during avascular growth and no therapy and $g(\Omega_\infty)$ represents the increase in tumour mass during vascular growth and no therapy.

Table 3
Combined therapy predictions of the model

Drugs combinations	Response	Profiles	Growth
Double			
AB; AC; AD	Clears tumour or arrests its growth	Fig. 3(b) and (c)	Fig. 7(a)
BC; BD; CD	Reduces tumour growth rate	Fig. 1(a) and (c)	Fig. 8(b)
Triple			
ABC, ABD, ACD	Clears tumour or arrests its growth	Fig. 3(b) and (c)	Fig. 7(b)
BCD	Reduces tumour growth rate	Fig. 1(a) and (c)	Fig. 8(b)
Quadruple			
ABCD	Clears tumour or arrests its growth	Fig. 3(b) and (c)	Fig. 7(b)

(Δ_1, Δ_2, Δ_3, Δ_4 and Δ_5) as well as their rates of uptake (β_1, β_2, β_3, β_4, and β_5). We use the results from Sections 4–6 to fix these parameters at values which, when each drug is given in isolation, correspond to effective treatment and investigate how the overall tumour growth dynamics change when different combinations of the therapies are administrated.

Our numerical simulations suggest that two qualitative outcomes are possible. In one case tumour invasion of the host cells is controlled: the tumour is either cleared or becomes growth-arrested; in the other case, the tumour vasculature is destroyed and the tumour becomes avascular. The former case is the same as that for effective treatment with drug A only, whilst the latter is the same as that for effective antiVEGF therapy (drug B), effective antivascular therapy (combined drugs C and D) or effective combinations of drugs B, C and D.

We predict that combined therapy prevents tumour invasion, leading to tumour arrested growth or tumour clearance, only when one of the drugs in the cocktail kills proliferating cells i.e. is drug A. If a combination of the drugs B, C and D is applied, tumour growth is slowed (see Fig. 7(b)) but invasion persists. In Table 3 we summarize the different responses that can be achieved when different combinations of the drugs are administrated.

We recall that the aim of an ideal treatment is to clear all tumour cells whilst inflicting no damage on the normal cells. Our results in Table 3 suggests that the tumour is cleared under the influence of a treatment with drug A only or a combination of drug A with drugs B, C or D. The time when the tumour is removed depends on the parameter Δ_2 that controls the potency of the drug A on the tumour cells. In order to compare how quickly the tumour is removed under different therapy scenarios, in Fig. 8(a) and (b) we plot the clearance time T upon application of different therapies Ω as $T(\Omega)$[2] with the change in Δ_2. We summarize our results as follows:

$$T(AB) < T(A) < T(AC) < T(AD), \tag{19}$$

$$T(ABC) < T(AB) < T(A) < T(AC) < T(ABD) < T(ACD) < T(ABCD) < T(AD). \tag{20}$$

Our results predict that when applying a double therapy the tumour is removed quickest with a treatment that kills tumour proliferating cells (drug A) and reduces the influence of the VEGF in the region (drug B). The clearance of the tumour is slowest when the therapy targets the proliferating cells (drug A) and kills the blood vessels (drug D).

Upon application of combined triple and quadruple therapies the therapy removes the tumour in shortest time when the combined therapy reduces VEGF influence (drug B) and kills the angiogenic capillaries (drug C) in parallel with targeting proliferating cells (drug A). The tumour will take longest to be removed under a combined therapy that destroys the blood vessels (drug D) in combination with killing proliferating cells (drug A).

Following different therapies with isolated or combined drugs A, B, C and D, some damage can be sustained by the normal cells. In our numerical simulations this is represented by a decrease in the overall density of the normal tissue and is evident only when drug D is administered in isolation or combined with drugs A, B and C. This is expected since upon delivery of the drug D the mature vasculature is destroyed resulting in absence of oxygen delivery to the healthy tissue. As a consequence the region becomes hypoxic and whilst tumour cells may survive healthy tissue is not viable. Therefore our results predict potential strongly deleterious effects on the healthy cells following a successful therapy that includes drug D.

---

[2] As in Section 7 Ω represents different therapies with drugs A, B, C and/or D.
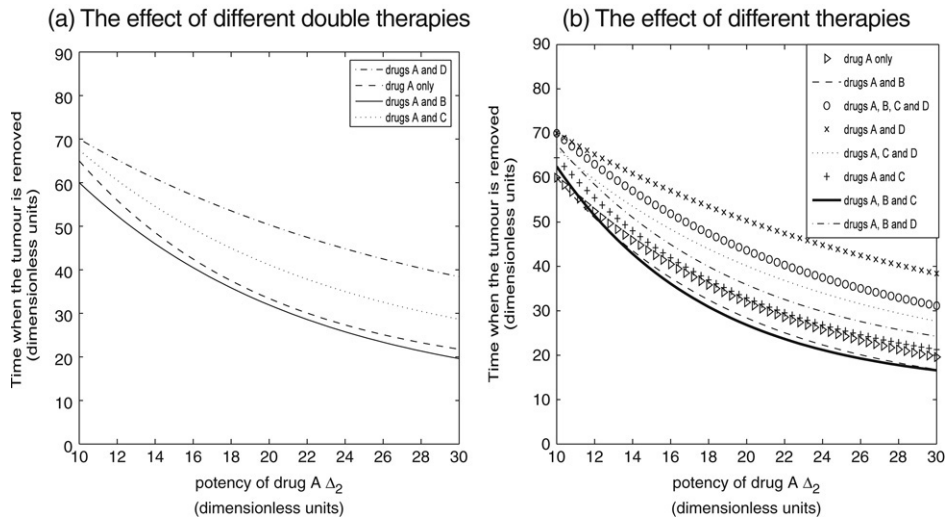
Fig. 8. (a) Numerically calculated time when the tumour is removed T_R as a result of combining drug A which kills proliferating cells with drugs B, C and D which destroy the VEGF or the tumour vasculature. To calculate this time we solve (7)–(16) for different values of Δ_2 with the rest of the parameters as per Fig. 1 with $c_1 = 10$, $c_2 = 5$, $\Delta_1 = 2$, $\beta_2 = 1$. Our results suggest that the tumour is removed quicker when the potency effect of the antiproliferative drug (measured by Δ_2) is larger. A combination of drug A with drug B removes the tumour quickest. (b) The numerically calculated time when the tumour is removed as a result of application of different triple or quadruple therapies by delivery of combinations of drug A with drugs B, C and/or D.

When we exclude administration of drug D, the most effective treatment that removes the tumour (see Fig. 8(a) and (b)) is a combination of drugs A, B and C which for given drug potency clears the tumour at shortest time. In contrast the most effective treatment that controls vascular tumour growth is combination of drugs B and C, upon which application the increase in tumour mass is least (see Fig. 7(a) and (b)).

9. Discussion

In this paper we extended a model formulated in [28] to investigate the response of a vascular tumour to treatment with different anticancer drugs. Our results suggest that the tumour's response to a therapy that kills proliferating tumour cells (drug A) depends on its potency and rate of uptake by the tumour cells. In particular, at long time the vascular tumour will either be cleared, become growth-arrested or will grow at a reduced rate, depending on the values of the relevant model parameters (see Fig. 3(a)–(c)).

When VEGF or the tumour vasculature are targeted by drugs of type B or C or D, tumour elimination can not occur. Instead, at best vascular growth is retarded (see Fig. 7(a) and (b)). Upon application of combined antivascular therapy the results are qualitatively the same as if isolated antiVEGF or antivascular therapy were effective: the tumour reverts to avascular growth but cannot be eliminated. Combining anti-proliferative therapy with antiVEGF or antivascular therapy can eliminate a vascular tumour in our simulations. For different combinations of the drugs of type A with drugs B, C and/or D the time of tumour removal depends on the potency of the drug that kills the proliferating tumour cells (see Fig. 8(a) and (b)).

The results in this paper are of clinical relevance. What we suggest via our modelling is different from the conventionally used treatment methods where one therapy is applied followed by another therapy after some time interval. Our combination therapy includes simultaneous application of a cocktail of drugs targeting different aspects of tumour growth at the same time. We predict that a cocktail of drugs that kill the proliferating tumour cells, reduce the VEGF and destroy the angiogenic capillaries will remove the tumour in shortest time whilst inflicting no damage on the healthy tissue, whilst a combination of only antivascular and antiVEGF drugs can, at best, reduce the vascular tumour's growth rate to that of its avascular counterpart.

Combination therapy is currently used in controlling the growth and spread of the HIV virus and the development of AIDS [54]. This motivated us to explore whether combination anticancer therapy will be more effective then single anticancer therapy. Recently combination therapies have been suggested for use in treating breast cancer [39,42].

Using a virtual cancer patient engine Agur et al. [39] studied short- and long-term cellular dynamics of specific patients undergoing drug therapy with only doxorubicin or a doxorubicin combined treatments. Their results for the therapy outcomes for individual patients agree with *in vitro* response to doxorubicin protocols, and offer per-case choice of drug, drug combination and schedules to achieve desired clinical end points [39]. Fister and Panetta [43] reviews the use of mathematical models to study breast cancer chemotherapy and illustrates the relationship between different therapies and the initiation time of metastatic growth, predicting the effect of the therapy on the metastatic growth and suggests the optimal chemotherapy administration. With our model, we have used a much simpler mathematical framework than that in [39,43] and studied continuous infusion of the combined drugs making theoretical predictions. Questions remain whether the suggested therapies are feasible and whether the associated side effects can be tolerated.

A weakness of our modelling framework which underplays the efficacy of some of the treatments studied is its inability to give rise to an avascular steady state solution. The modelling framework developed here can be extended to include necrotic material production by the hypoxic cells and its degradation, which would give rise to avascular tumour arrested growth. The model developed here also leads naturally to several possibilities for further investigation. For example, our model can be extended to study more sophisticated treatment strategies such as two-step targeting of multi-cell type tumours [52]. This would allow us to determine conditions for which one strategy is better than another. We could also extend our work to account for treatment with drugs that target different phases of the cell cycle by extending the work of Pettet et al. [55]. However, for the purpose of this paper we have studied three different isolated treatments for controlling vascular tumour growth, as well as their combination. We have proposed theoretical results of the effectiveness of such treatments which we hope will be tested clinically in future.

Acknowledgements

References

 [1] J.J. Casciari, S.V. Sotirchos, R.M. Sutherland, Variations in tumour growth rates and metabolism with oxygen concentration, glucose concentration and extracellular pH, J. Cell. Physiol. 151 (1992) 386–394.
 [2] R.M. Sutherland, Cell and environment interactions in tumour microregions: The multicell spheroid model, Science 240 (1988) 177–184.
 [3] V.R. Muthukkaruppan, L. Kubai, R. Auerbach, Tumour-induced neovascularisation in the mouse eye, J. Natl. Cancer Inst. 69 (1982) 699–705.
 [4] J. Baptist-Trimbos, P. Trimmers, Chemotherapy for early ovarian cancer, Curr. Opin. Obstet. XC Gyn. 16 (1) (2004) 43–48.
 [5] www.cancer.org/docroot/ETO/content/ETO12XSurgery.asp.
 [6] http://www.breastcancer.org/treatment/radiation/index.jsp.
 [7] http://www.hopkinsmedicine.org/radiosurgery/disorders/braintumors.cfm.
 [8] www.pbs.org/wgbh/nova/cancer/treatments.htm.
 [9] J.C. Cheng, V.P. Chuang, S.H. Cheng, A.T. Huang, Y. Lin, T. Cheng, P. Yang, D. You, J.J. Jian, S.Y. Tsai, J. Sung, S. Horng, Local radiotherapy with or without transcatheter arterial chemoembolization for patients with unresectable hepatocellular carcinoma, Int. J. Rad. Oncol. Biol. Phys. 47 (2) (2000) 435–442.
[10] www.tirgan.com/chemolist.htm.
[11] http://home.attbi.com/apparat/articles/cancer.html.
[12] B.R. Stoll, C. Migliorini, A. Kadambi, L.L. Munn, R.K. Jain, A mathematical model of the contribution of endothelial progenitor cells to angiogenesis in tumours: Implications for anti-angiogenic therapy, Blood 102 (2003) 2555–2561.
[13] E.K. Rowinsky, R.C. Donehower, Paclitaxel (Taxol), N. Engl. J. Med. 223 (1995) 1004–1014.
[14] http://www.cancerguide.org/rcc_thalidomide.html.
[15] http://www.oxigene.com/vascular/combretastatin.asp?sf=t.
[16] J.A. Sherratt, M.A.J. Chaplain, A new mathematical model for avascular tumour growth, J. Math. Biol. 43 (2001) 291–312.
[17] J.P. Ward, J.R. King, Mathematical modelling of avascular-tumour growth II: Modelling growth saturation, IMA J. Math. Appl. Med. Biol. 16 (1999) 171–211.
[18] R.A. Gatenby, E.T. Gawlinski, A reaction–diffusion model of cancer invasion, Cancer Res. 56 (1996) 5745–5753.
[19] J.A. Sherratt, M.A. Nowak, Oncogenes, anti-oncogenes and the immune response to cancer: A mathematical model, Proc. R. Soc. Lond. 248 (1992) 261–271.
[20] A.R.A. Anderson, M.A.J. Chaplain, Continuous and discrete mathematical models of tumour-induced angiogenesis, Bull. Math. Biol. 60 (1998) 857–900.
[21] H.M. Byrne, M.A.J. Chaplain, Mathematical models for tumour angiogenesis-numerical simulations and non-linear wave solutions, Bull. Math. Biol. 57 (1995) 461–486.

[22] M.E. Orme, M.A.J. Chaplain, A mathematical model of the first steps of tumour-related angiogenesis: Capillary sprout formation and secondary branching, IMA. J. Math. Appl. Med. Biol. 13 (1996) 73–98.

[23] M.E. Orme, M.A.J. Chaplain, Two-dimensional models of tumour angiogenesis and anti-angiogenic strategies, IMA. J. Math. Appl. Med. Biol. 14 (1997) 189–205.

[24] C.J.W. Breward, H.M. Byrne, C.E. Lewis, A multiphase model describing vascular tumour growth, J. Math. Biol. 65 (2003) 609–640.

[25] C.J.W. Breward, H.M. Byrne, C.E. Lewis, Modelling the interaction between tumour cells and a blood vessel in micro-environment within a vascular tumour, Eur. J. Appl. Math. 12 (2001) 529–556.

[26] P. Hahnfield, D. Panigraphy, J. Folkman, L. Hlatky, Tumour development under angiogenic signalling: A dynamic theory of tumour growth, treatment response and post-vascular dormancy, Cancer Res. 59 (1990) 4770–4775.

[27] A. d'Onfrio, A. Gandolfi, Tumour eradication by anti-angiogenic therapy: Analysis and extension of the model by Hahnfeldt et al. (1999), Math. Biosci. 191 (2004) 154–184.

[28] Jasmina Panovska, Helen M. Byrne, Philip K. Maini, Mathematical modelling of vascular tumour growth and implications for therapy, in: A. Deutsch, L. Brusch, H. Byrne, G. de Vries, H.-P. Herzel (Eds.), Mathematical Modeling of Biological Systems, Vol. I, Birkhäuser, Boston, 2007, pp. 211–222.

[29] L. Griffiths, G.U. Daches, The influence of oxygen tension and pH on the expression of platelet-derived endothelial cell growth factor thymidine phosphorylase in human breast tumour cells *in vitro* and *in vivo*, Cancer Res. 57 (1997) 570–572.

[30] E. De Angelis, L. Preziosi, Advection–diffusion models for solid tumour evolution in vivo and related free boundary problems, Math. Models Methods Appl. Sci. 10 (2000) 379–407.

[31] L.T. Baxter, F. Yuan, R.K. Jain, Pharmacokinetic analysis of the perivascular distribution of bifunctional antibodies and haptens: Comparison with experimental data, Cancer Res. 525 (1992) 838–850.

[32] M.M. Sholley, G.P. Ferguson, Mechanism of neovascularization. Vascular sprouting can occur without proliferation of endothelial cells, Lab. Invest. 51 (1984) 624–634.

[33] M.S. O'Reilly, T. Boehm, Y. Shing, N. Fukai, G. Vasios, W.S. Lane, E. Flynn, J.R. Birkhead, B.R. Olsen, J. Folkman, Endostatin: An endogenous inhibitor of angiogenesis and tumour growth, Cell 88 (1997) 277–285.

[34] M.S. O'Reilly, L. Holmgren, Y. Shing, C. Chen, R.A Rosenthal, M. Moses, W.S. Lane, Y. Cao, E.H. Sage, J. Folkman, Angiostatin. A novel angiogenic inhibitor that mediates the suppression of metastasis by a Lewis lung carcinoma, Cell 79 (1994) 315–328.

[35] C.M. West, P. Price, Combretastatin A4 phosphate, Anticancer Drug. 15 (3) (2004) 179–187.

[36] J.P. Ward, J.R. King, Mathematical modelling of drug transport in tumour multicell spheroids and monolayer cultures, Math. Biosci. 181 (2003) 177–207.

[37] T.L. Jackson, H.M. Byrne, A mathematical model to study the effects of drug resistance and vasculature on the response of solid tumours to chemotherapy, Math. Biosci. 164 (2000) 17–38.

[38] L. Arakelyn, Y. Merbi, Z. Agur, Vessel maturation effects on tumour growth: Validation of a computer model in implanted human ovarian carcinoma spheroids, Eur. J. Cancer 41 (1) (2004) 159–167.

[39] Z. Agur, L. Arakelyan, G. Belilty, N. Dahan, H. Harpak, Y. Kogan, Y. Merbl, A. Rabinovich, M. Shoham, I. Ziv, Application of the Virtual Cancer Patient Engine (VCPE) for improving oncological treatment design, J. Clin. Oncol. 22 (14S) (2004) 692–700.

[40] J. Sinek, H. Frieboes, X. Zheng, V. Cristini, Two-dimensional chemotherapy simulations demonstrate fundamental transport and tumour response limitations involving nanoparticles, Biomed. Microdev. 6 (4) (2004) 297–309.

[41] X. Zheng, S.M. Wise, V. Cristini, Non-linear simulator of tumour progression and interaction with the vasculature via an adaptive finite-element/level-set method, Bull. Math. Biol. 67 (2) (2005) 211–259.

[42] K.R. Fister, J.C. Panetta, Optimal control applied to cell-cycle-specific cancer chemotherapy, SIAM J. Appl. Math. 60 (3) (2000) 1059–1072.

[43] K.R. Fister, J.C. Panetta, Optimal control applied to competing chemotherapeutic cell-kill strategies, SIAM J. Appl. Math. 63 (6) (2003) 1954–1971.

[44] D. Balding, D.L.S. McElwain, A mathematical model of tumour-induced capillary growth, J. Theor. Biol. 114 (1985) 53–73.

[45] L. Edelstein, L.A. Segel, Growth and metabolism in mycelial fungi, J. Theor. Biol. 104 (1983) 187–210.

[46] J. Panovska, Mathematical modelling of tumour growth and applications for therapy, D.Phil Thesis, Oxford University, UK, 2005.

[47] C.L. Stokes, D.A. Lauffenburger, Analysis of the roles of microvessel endothelial cell random motility and chemotaxis in angiogenesis, J. Theor. Biol. 152 (1991) 377–403.

[48] W.H. Press, S.A. Teukolsky, W.T. Vetterling, B.P. Flannery, Numerical Recepies in Fortran: The Art of Scientific Computing, 2nd ed., Cambridge University Press, 1994.

[49] M. Degregorio, G. Lui, B. Macher, J. Wilbur, Uptake, metabolism and cytotoxicity of doxorubicin in human ewing's carcinoma and rhabdomysarcoma cells, Cancer Chemo. Pharmacol. 12 (1984) 59–70.

[50] T.L. Jackson, Intracellular accumulation and mechanism of action of doxorubicin in a spatio-temporal tumour model, J. Theor. Biol. 220 (2002) 210–213.

[51] M. Dordel, J.N. Winter, A.J. Atkinson, Kinetic analysis of P-glycoprotein-mediated doxorubicin effect, J. Pharmacol. Exp. Ther. 263 (1992) 762–780.

[52] T.L. Jackson, Vascular tumour growth and treatment: Consequences of polyclonality, competition and dynamic vascular support, J. Math. Biol. 44 (3) (2002) 201–226.

[53] K.R. Laderoute, R.M. Alarcon, Opposing effects of hypoxia on expression of the angiogenic inhibitor thrombospondin 1 and angiogenic inducer vascular endothelial growth factor, Clin. Cancer Res. 6 (2000) 2941–2950.

[54] http://www.hivandhepatitis.com/recent/virologic/011405_a.html.

[55] G.J. Pettet, C.P. Please, M.J Tindall, D.L.S. McElwain, The migration of cells in multicell tumour spheroids, Bull. Math. Biol. 63 (2001) 231–257.